

Three-Point Energy Correlator in $\mathcal{N} = 4$ Supersymmetric Yang-Mills Theory

Kai Yan^{1,2} and Xiaoyuan Zhang³

¹INPAC, Shanghai Key Laboratory for Particle Physics and Cosmology, School of Physics and Astronomy, Shanghai Jiao Tong University, Shanghai 200240, China

²Key Laboratory for Particle Astrophysics and Cosmology (MOE), Shanghai 200240, China

³Harvard University, Cambridge, Massachusetts 02138, USA

 (Received 23 March 2022; accepted 7 June 2022; published 6 July 2022)

An analytic formula is given for the three-point energy correlator at leading order in maximally supersymmetric Yang-Mills theory ($\mathcal{N} = 4$ sYM). This is the first analytic calculation of a three-parameter event shape observable, which provides valuable data for various studies ranging from conformal field theories to jet substructure. The associated class of functions define a new type of single-valued polylogarithms characterized by 16 alphabet letters, which manifest a $D_6 \times Z_2$ dihedral symmetry of the event shape. With the unexplored simplicity in the perturbative structure of the three-point energy correlator, all kinematic regions including collinear, squeezed and coplanar limits are now available.

DOI: [10.1103/PhysRevLett.129.021602](https://doi.org/10.1103/PhysRevLett.129.021602)

Introduction.—The energy correlator observable measures the energy deposited in multiple detectors as a function of angles between the detectors. From the phenomenological perspective, energy correlators probe the energy flow and can be used as jet observables [1–6] for precise tests of the standard model or new physics search. From the practical side, energy correlators are perhaps the simplest infrared safe event shape [7,8] to calculate analytically. From the theory side, they belong to class of observables probing the spatial correlation among flow operators, which provides valuable data for understanding the nature of quantum field theories [9–11].

The two-point energy correlator [12] is computed analytically to next-to-leading order in quantum chromodynamics (QCD) [13,14] and next-to-next-to-leading order in $\mathcal{N} = 4$ supersymmetric Yang-Mills theory (sYM) [15,16], numerically up to next-to-next-to-leading order in QCD [17–26], and resummed to all orders in both the back-to-back [27–32] and collinear limit [33–35]. Meanwhile the precision study on multiparticle energy correlator has been initiated, featuring the leading order prediction for the three-point energy correlator (EEEC) in the triple-collinear limit [36].

The EEEC, which depends on three angles among the detectors, captures the nontrivial shape dependence in the scattering processes. The standard definition for the EEEC as a differential cross section can then be recast as a five-point correlation function:

$$\begin{aligned} \text{EEEC}(\chi_1, \chi_2, \chi_3) &= \int \prod_{i=1}^3 [d\Omega_{\vec{n}_i} \delta(\vec{n}_i \cdot \vec{n}_{i+1} - \cos \chi_i)] \\ &\times \frac{\int d^4x e^{iqx} \langle 0 | O^\dagger(x) \mathcal{E}(\vec{n}_1) \mathcal{E}(\vec{n}_2) \mathcal{E}(\vec{n}_3) O(0) | 0 \rangle}{(q^0)^3 \int d^4x e^{iqx} \langle 0 | O^\dagger(x) O(0) | 0 \rangle}. \quad (1) \end{aligned}$$

Here, the detector operator that measures the energy flux in the direction \vec{n} is given by an integrated stress-energy tensor $T_{\mu\nu}$ [9,37–40], $\mathcal{E}(\vec{n}) = \int_{-\infty}^{\infty} d\tau \lim_{r \rightarrow \infty} r^2 n^i T_{0i}(t = \tau + r, r\vec{n})$. The operators O (source) and O^\dagger (sink) create the final state, whose particles are detected by the two calorimeters. The choice of the local operator O depends on the physical problem. For e^+e^- annihilation, O is given by an electromagnetic current.

The energy correlator is an on-shell observable that bears close relations to the off-shell correlation functions involving the stress-energy tensors. In view of this property, previous studies in $\mathcal{N} = 4$ sYM theory employed various shortcuts to obtaining the two-point energy correlator by taking multiple discontinuities of Euclidean correlation functions and by exploiting the superconformal symmetries of the latter [15,16,41–43]. It remains unknown whether such approaches are feasible for computing the higher-point energy correlators. In this Letter, we adopt an on-shell approach to obtain the EEEC from the super form factor for protected scalar operator [44,45], benefiting from the simplicity of matrix elements in $\mathcal{N} = 4$ sYM. We present the one-loop EEEC result for arbitrary angles, which is the first analytic calculation of multiparticle correlation observables with full shape dependence.

Our result encodes valuable information on the function space of the EEEC in perturbative quantum field theory: the classifications of symmetries, symbol alphabets, and

Published by the American Physical Society under the terms of the [Creative Commons Attribution 4.0 International license](https://creativecommons.org/licenses/by/4.0/). Further distribution of this work must maintain attribution to the author(s) and the published article's title, journal citation, and DOI. Funded by SCOAP³.

polylogarithms. These mathematical structures are studied much more thoroughly in the context of scattering amplitudes than finite observables in collider experiments. We are strongly motivated to initiate the discussion on these topics for the energy correlator observable, starting from $\mathcal{N} = 4$ sYM, as they provide powerful tools and experience for QCD [46], which is phenomenologically relevant for the cutting edge studies at LHC.

EEEC from four-point form factor.—In $\mathcal{N} = 4$ sYM, we may choose the source and sink to be scalar operators that are the bottom component of the supermultiplet of conserved currents. As such, they are natural analogs of the electromagnetic current, and have fixed conformal weight 2. The matrix element for producing a given on-shell superstate from the vacuum defines the so-called form factor [47–51]

$$\int d^4x e^{iq \cdot x} \langle X | O(x) | 0 \rangle \equiv (2\pi)^4 \delta^4(q - p_X) F_X. \quad (2)$$

In perturbative theories, EEEC can be obtained from the squared form factor by performing a weighted sum over the on-shell external states. For convenience, we normalize the event shape by a volume factor of the phase space, thus defining a function H through $\text{EEEC}(\chi_1, \chi_2, \chi_3) \equiv (8\pi^2) \times \|\vec{n}_1 \wedge \vec{n}_2 \wedge \vec{n}_3\|^{-1} H(\vec{n}_1, \vec{n}_2, \vec{n}_3)$, which we can evaluate by carrying out the on-shell phase-space integration while fixing the directions of three particles in the final states

$$H(\vec{n}_1, \vec{n}_2, \vec{n}_3) = \frac{1}{\sigma_{\text{tot}}} \sum_{(i,j,k) \in X} \int d\Pi_X \delta^2(\vec{n}_1 - \hat{p}_i) \times \delta^2(\vec{n}_2 - \hat{p}_j) \delta^2(\vec{n}_3 - \hat{p}_k) \frac{E_i E_j E_k}{(q^0)^3} |F_X|^2, \quad (3)$$

where i, j , and k run over all final-state particles. H has the perturbative expansion $H = \sum_{k \geq 1} a^k H^{(k)}$ in the 't Hooft coupling. The born level event shape is a delta function due to 3-body kinematic constraints, $H_{\text{Born}} = \delta(\|\vec{n}_1 \wedge \vec{n}_2 \wedge \vec{n}_3\|) \text{csc}^2(\chi_1/2) \text{csc}^2(\chi_2/2) \text{csc}^2(\chi_3/2)$. The leading order that has nontrivial three-angle dependence is $\mathcal{O}(a^2)$, where the complication comes from the tree-level four-point next-to-maximally-helicity-violating supermatrix elements $|F_4|^2$; for details, see [52,53]. After summing over superstates and symmetrization over the final-state momenta, the squared four-point form factor can be organized into a concise form:

$$|F_4|_{\text{sym}}^2 = \frac{q^4}{s_{12}s_{23}s_{34}s_{41}} \left[\frac{1}{4} + \frac{s_{23}s_{41}}{s_{341}s_{412}} + \frac{s_{23}s_{34}}{s_{123}s_{341}} \right] + \text{perm}(1, 2, 3, 4), \quad (4)$$

where the second and third term in the bracket correspond to the next-to-maximally-helicity-violating contribution.

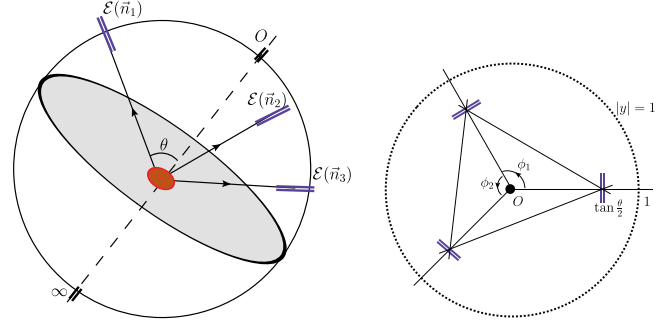


FIG. 1. Graphical representation of the three-point energy correlator: particles produced out of the vacuum by the source are captured by the three detectors located at spatial infinity in the directions of the unit vectors \vec{n}_1, \vec{n}_2 , and \vec{n}_3 . They can be mapped onto three points located on a circle with radius $|y| = \tan(\theta/2)$ on the celestial sphere. The three angles are parametrized by $[\sin(\chi_1/2), \sin(\chi_2/2), \sin(\chi_3/2)] = \sin \theta [\sin(\phi_1/2), \sin(\phi_2/2), \sin(\phi_1 + \phi_2)/2]$.

To compute the EEEC, we first apply topology identification to the squared matrix elements. With the EEEC measurement functions, they can be decomposed into four topologies. To proceed, we parametrize the kinematic invariants by the energy fractions of three detected final-state particles as well as the three angles (θ, ϕ_1, ϕ_2) as depicted in Fig. 1. In particular, we switch to the following set of angle parameters,

$$s = \tan^2 \frac{\theta}{2}, \quad \tau_1 = e^{i\phi_1}, \quad \tau_2 = e^{i\phi_2}, \quad (5)$$

such that both the matrix elements and phase space simplify down. Integrating the four-particle phase space [54] against the measurement functions, we are left with a set of twofold integrals that are linearly reducible [55–58], which allows us to compute directly in HYPERINT [59].

Symbol alphabets.—The EEEC can be expressed in a frame independent manner as a function of three conformally invariant variables:

$$\zeta_{ij} = \frac{q^2(p_i \cdot p_j)}{2(q \cdot p_i)(q \cdot p_j)} = \frac{\langle p_i p_j \rangle \langle \xi_j \xi_i \rangle}{\langle p_i \xi_i \rangle \langle p_j \xi_j \rangle}, \quad |\xi_j\rangle \equiv q|j\rangle. \quad (6)$$

From the results of function H , we read off 16 symbol alphabets, which contain two types of algebraic roots,

$$|\Delta_1| \equiv \|\vec{n}_1 \wedge \vec{n}_2 \wedge \vec{n}_3\| = \sqrt{(1 - u_1 - u_2 - u_3)^2 - 4u_1 u_2 u_3} \\ |\Delta_2| \equiv \|\vec{n}_1 \wedge \vec{n}_2 + \vec{n}_2 \wedge \vec{n}_3 + \vec{n}_3 \wedge \vec{n}_1\| = \sqrt{\lambda(\zeta_{12}, \zeta_{23}, \zeta_{31})},$$

where $\{u_i\} \equiv \{1 - \zeta_{ij}\}$ and $\lambda(a, b, c) \equiv a^2 + b^2 + c^2 - 2ab - 2ac - 2bc$ is the Källén function.

The representation of variables in Eq. (6) foreshadows a D_6 dihedral symmetry of the EEEC, which can be better visualized as we embed the kinematic data $|p_i\rangle \equiv |2i - 1\rangle, |\xi_i\rangle \equiv |2i + 2\rangle$ in a 2×6 matrix Z : $Z_a = |a\rangle \in CP^1$,

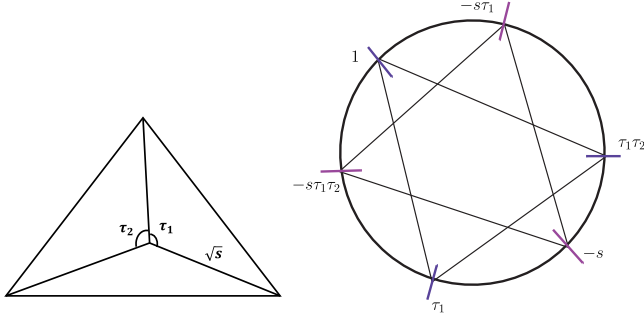


FIG. 2. Embedding of the EEEC kinematics. Left: Three points on the celestial sphere that we put on a unit circle with radius \sqrt{s} centered at the origin. Right: Realization of this kinematic configuration as a hexagon located on a unit circle.

$$Z \doteq \begin{pmatrix} 1 & 1 & 1 & 1 & 1 & 1 \\ \eta_1 & \eta_2 & \eta_3 & \eta_4 & \eta_5 & \eta_6 \end{pmatrix}, \quad \eta_a - \eta_b \doteq \frac{\langle ab \rangle}{\langle a\infty \rangle \langle \infty b \rangle}, \quad (7)$$

where $|\infty\rangle = (0, 1)^T$.

The geometric interpretation of the above formalism is clear in the center of mass frame where $q = (q^0, 0, 0, 0)$, so that under stereographic projection the three vectors \vec{p}_i are mapped onto a triangle $(y_i, \bar{y}_i) = (\eta_i, -1/\eta_{i+3})$ on the celestial sphere. Let us further introduce a special point $(y_I, \bar{y}_I) = (\eta_I, -1/\eta_I)$ representing the center of the triangle, whose location determined by the equation

$$\frac{\langle 1I \rangle \langle 4\bar{I} \rangle \langle 52 \rangle}{\langle 14 \rangle \langle 2\bar{I} \rangle \langle 5I \rangle} = \frac{\langle 3I \rangle \langle 6\bar{I} \rangle \langle 14 \rangle}{\langle 36 \rangle \langle 1I \rangle \langle 4\bar{I} \rangle} = 1. \quad (8)$$

We may impose $|I\rangle = (0, 1)^T$, $|\bar{I}\rangle = (1, 0)^T$ and $\langle \bar{I}1 \rangle = \langle aI \rangle = 1$, and expand the kinematic space to include I (or equivalently \bar{I}). Thus, we fix the gauge under which

$$Z|I\rangle = \begin{pmatrix} 1 & 1 & 1 & 1 & 1 & 1 & 0 \\ 1 & -s\tau_1\tau_2 & \tau_1 & -s & \tau_1\tau_2 & -s\tau_1 & 1 \end{pmatrix}. \quad (9)$$

The kinematic space is mapped onto two similar triangles whose circumcenter sit at the origin, which we display as a hexagon located on a unit circle (see right panel of Fig. 2).

In this way, we identify all 16 EEEC alphabets with products of Plücker variables $\langle ab \rangle$, $\langle aI \rangle$ as well as certain homogeneous polynomials in the form

$$d_{(ab)(cd)(ef)} \equiv \langle ad \rangle \langle eb \rangle \langle cf \rangle - \langle af \rangle \langle cb \rangle \langle ed \rangle. \quad (10)$$

Switching variables into three conformally invariant ratios,

$$y = -\frac{\langle 31 \rangle \langle 5I \rangle}{\langle 15 \rangle \langle I3 \rangle}, \quad z = -\frac{\langle 13 \rangle \langle 56 \rangle}{\langle 35 \rangle \langle 61 \rangle}, \quad w = \frac{\langle 51 \rangle \langle 62 \rangle \langle 43 \rangle}{\langle 35 \rangle \langle 16 \rangle \langle 24 \rangle},$$

we could transform the alphabets into 16 polynomials with all positive signs, which read

$$\begin{aligned} & \{w, 1+w, y, 1+y, z, 1+z, w+z, 1+w+z, \\ & y+z+yz, w+y+z+yz, 1+w+z+yz, \\ & 1+w+y+2z+yz, y+wy+y^2+z+2yz+y^2z, \\ & 1+y+wy+y^2+z+2yz+y^2z, \\ & 1+w+y+wy+y^2+z+2yz+y^2z, \\ & 1+w+y+wy+y^2+2z+2yz+y^2z\}. \end{aligned} \quad (11)$$

Symmetries and functional basis.—Within our embedding formalism, the EEEC exhibits a set of discrete symmetries. First, we have D_6 dihedral symmetries acting on the hexagon coordinates $Z_a (a+6 \doteq a)$, which are generated by dihedral flip $\tau: a \xrightarrow{\tau} 4-a$, cyclic permutation $\sigma: a \xrightarrow{\sigma} a+2$, and parity conjugation $P: a \xrightarrow{P} a+3$. In addition, there is a residual Z_2 symmetry corresponding to the exchange between two solutions to Eq. (8). It is generated by an operation that we call reflection $R: (\langle Ia \rangle / \langle Ia+2 \rangle) \xrightarrow{R} [(\langle aa+3 \rangle \langle Ia+5 \rangle) / (\langle a+2a+5 \rangle \langle Ia+3 \rangle)]$. P and R flip the signs of Δ_1 and Δ_2 , respectively, such that $\Delta_1 \xrightarrow{P} -\Delta_1$, $\Delta_1 \xrightarrow{R} \Delta_1$, while $\Delta_2 \xrightarrow{P} \Delta_2$, $\Delta_2 \xrightarrow{R} -\Delta_2$.

In light of these properties, we are ready to lift the one-loop symbols into polylogarithmic functions. To start, we shall identify a set of variables S that is closed under $\{\tau, \sigma, P, R\}$, such that $\{S, 1+S\}$ factorize into polynomials that cover the EEEC alphabet letters in Eq. (11).

Let us introduce these variables. For clarity, we switch to a different gauge by performing a $GL(2) \times GL(1)^6$ transformation on Eq. (9),

$$Z|I\rangle = \begin{pmatrix} 1 & 1 & 1 & 0 & 1 & 1 & 1 \\ 0 & \frac{1}{1+x_1} & 1 & -1 & -x_2 & -\frac{x_2 x_3}{1+x_3} & \frac{1+x_4}{x_4} \end{pmatrix}, \quad (12)$$

thus introducing four parameters (x_1, x_2, x_3, x_4) , three of which are independent.

Notice that the hexagon Z corresponds to the Grassmannian $\text{Gr}(2, 6)/[GL(1)]^5$, which can be associated with a A_3 -cluster algebra, with a quiver being (x_1, x_2, x_3) . Given this observation, we introduce 15 conformally invariant ratios to cover the full set of \mathcal{X} coordinates [60,61], namely

$$w_3 = x_1 = \frac{\langle 23 \rangle \langle 14 \rangle}{\langle 12 \rangle \langle 34 \rangle}, \quad z_3 = x_2 = \frac{\langle 34 \rangle \langle 15 \rangle}{\langle 13 \rangle \langle 45 \rangle}, \quad (13)$$

$$\begin{aligned} v_2 &= \frac{1+x_3}{x_2 x_3} = \frac{\langle 46 \rangle \langle 13 \rangle}{\langle 34 \rangle \langle 16 \rangle}, \\ w_3 \xrightarrow{P} \bar{w}_3 &= \frac{\langle 14 \rangle \langle 56 \rangle}{\langle 45 \rangle \langle 16 \rangle}, \quad z_3 \xrightarrow{P} \bar{z}_3 = \frac{\langle 16 \rangle \langle 24 \rangle}{\langle 46 \rangle \langle 12 \rangle}, \end{aligned} \quad (14)$$

as well as their images under cyclic permutations.

In addition, we introduce $r_1 = 1/x_4 = -[(\langle 14 \rangle \langle 3I \rangle) / (\langle 13 \rangle \langle 4I \rangle)]$, whose images under D_6 transformations form a set of 12 cross ratios:

$$r_a = \frac{\langle aa+3 \rangle \langle a+2I \rangle}{\langle aa+2 \rangle \langle Ia+3 \rangle}, \quad \bar{r}_a = \frac{\langle a+5a+2 \rangle \langle a+3I \rangle}{\langle a+5a+3 \rangle \langle Ia+2 \rangle}, \quad (15)$$

satisfying $r_a \xrightarrow{P} r_{a+3}, r_a \xrightarrow{R} \bar{r}_a, a+6 \doteq a$.

In terms of these ingredients, we can define $S \equiv \{r_1, w_1, z_1, v_1, -w_1/\bar{w}_1, -|z_1|^2\}$ plus their D_6 images and conclude that it has the desired properties, i.e., $\text{Li}_{1,2}(-S)$ (modulo products of logarithms) account for the one-loop symbol letters for the EEEEC.

Next we investigate the structures of physical singularities, leading to a set of first-entry conditions that further constrain the function space: (i) single valueness in the physical domain away from the coplanar limit: for $|\tau_1| = |\tau_2| = 1, |s| < 1$ (or $|s| > 1$), the function must be free from ambiguity in the principal values of azimuthal angles, i.e., invariant as $\tau_1 \rightarrow e^{\pm 2\pi i} \tau_1, \tau_2 \rightarrow e^{\pm 2\pi i} \tau_2$; (ii) near triple-collinear limit: the function is free from logarithmic singularity in the triple-collinear limit as $s \rightarrow 0$ or ∞ .

As a consequence, only 6 independent letters drawn from the set $\{(\bar{w}_1/w_1) = \prod_{i=1}^3 [(1+w_i)/(1+\bar{w}_i)], |z_i|^2 = [v_i/(v_{i+1}), 1+v_i]\}$ can appear in the first entry. In particular, a parity odd letter $(\bar{w}_1/w_1) = \{[(s+\tau_1)(s+\tau_2)(1+s\tau_1\tau_2)]/[(1+s\tau_1)(1+s\tau_2)(s+\tau_1\tau_2)]\}$ is allowed, which distinguishes the EEEEC function space from the standard single-valued polylogarithms [62].

In conclusion, the one-loop EEEEC function space comprises classical polylogarithms whose arguments are drawn from the set $\{-S, 1+S\}$ satisfying the first-entry conditions. We observe that the final answer can be decomposed onto 14 such functions as well as their cyclic permutations. Hence, the one-loop EEEEC in $\mathcal{N} = 4$ sYM can be written in the a form that has manifest D_6 symmetry:

$$H_{\mathcal{N}=4}^{\text{LO}}(\vec{n}_1, \vec{n}_2, \vec{n}_3) = \sum_{i=1}^{14} b_i F_i + \text{perm}(\vec{n}_1, \vec{n}_2, \vec{n}_3), \quad (16)$$

where \vec{b} is a set of rational functions of (s, τ_1, τ_2) , \vec{F} contains weight-1 and weight-2 polylogarithmic functions. More explicitly,

$$\vec{F} \equiv \{f_1, f_2, f_3, g_1, \dots, g_{11}\}. \quad (17)$$

Each member of \vec{F} has a distinct signature under the operation τ and P , where $\{f_1, f_2, g_{2-4}, g_{8-11}\}$ and $\{f_1, g_3, g_4, g_7, g_9\}$ are odd under τ and P , respectively. The first three members $f_{1,2,3}$ are weight-1 functions:

$$f_1 = \ln \frac{\bar{w}_1}{w_1}, \quad f_2 = \ln |z_2|^2, \quad f_3 = \ln(1+v_2). \quad (18)$$

The rest, g_{1-11} are weight-2 functions, among which g_{1-8} are characterized by the 9 A_3 -cluster alphabets, depending only on $\{w_i, z_i, v_i\}$ and their parity conjugation:

$$\begin{aligned} g_1 &= \text{Li}_2(-v_2) \\ g_2 &= \text{Li}_2(1+w_3) + \text{Li}_2(1+\bar{w}_3) + 2\text{Li}_2(-v_3) \\ &\quad - \text{Li}_2(1+w_1) - \text{Li}_2(1+\bar{w}_1) - 2\text{Li}_2(-v_1) \\ g_3 &= \text{Li}_2(-z_2) - \text{Li}_2(-\bar{z}_2) + \frac{1}{2} \ln |z_2|^2 \ln \frac{1+z_2}{1+\bar{z}_2} \\ g_4 &= \text{Li}_2(1+w_1) - \text{Li}_2(1+\bar{w}_1) + \text{Li}_2(1+w_2) \\ &\quad - \text{Li}_2(1+\bar{w}_2) + \text{Li}_2(1+w_3) - \text{Li}_2(1+\bar{w}_3) \\ g_5 &= \pi^2 \quad g_6 = \ln^2 \frac{\bar{w}_1}{w_1} \quad g_7 = \ln \frac{\bar{w}_1}{w_1} \ln |z_2|^2 \\ g_8 &= \ln(1+v_3) \ln |z_1|^2 - \ln(1+v_1) \ln |z_3|^2. \end{aligned} \quad (19)$$

g_{11} is the only member depending on $\{r_i\}$, and the only one exhibiting an odd Z_2 signature, $g_{11} \xrightarrow{R} -g_{11}$:

$$g_{11} = \sum_{i=1}^6 \text{Li}_2(-r_i) - \text{Li}_2(-\bar{r}_i) + \frac{1}{2} \ln |r_i|^2 \ln \frac{1+r_i}{1+\bar{r}_i}. \quad (20)$$

The last two members, $g_{9,10}$, are responsible for the homogeneous polynomials that appear as alphabet letters, namely $\langle 12 \rangle \langle 34 \rangle \langle 56 \rangle - \langle 32 \rangle \langle 54 \rangle \langle 16 \rangle, \langle 54 \rangle \langle 12 \rangle \langle 36 \rangle - \langle 14 \rangle \langle 32 \rangle \langle 56 \rangle$:

$$g_9 = \frac{1}{2} \text{Li}_2 \left(1 - \frac{\bar{w}_1}{w_1} \right) - \frac{1}{2} \text{Li}_2 \left(1 - \frac{w_1}{\bar{w}_1} \right) \quad (21)$$

$$g_{10} = \text{Li}_2(1-|z_2|^2) + \frac{1}{2} \ln |z_2|^2 \ln |1-z_2|^2. \quad (22)$$

In the ancillary files, we provide the explicit expressions for the coefficients \vec{b} , as well as the full analytic expression for $H_{\mathcal{N}=4}^{\text{LO}}$ in terms of the ζ_{ij} -variables. In Fig. 3, we display the function H in various kinematic regions.

Special kinematics.—In the EEEEC, physical singularities emerge on the surfaces in the three-dimensional parameter space displayed in Fig. 4. Our rational parametrization, Eq. (5), makes it easy to access the three types of singular regions where the EEEEC is enhanced, namely the limit where three detectors are collinear ($s \rightarrow 0$ or ∞), two of them are collinear ($\tau_2 \rightarrow 1$), or the three detectors are coplanar ($s \rightarrow 1$). We extract analytically the leading power asymptotic behaviours in all these limits.

The ‘‘triple-collinear limit’’ describes single jet events where the all three angles are small $\zeta_{ij} \sim 0$. Taking $s \rightarrow 0$, we verify that it is a regular limit free from logarithmic enhancement, such that $H \sim (1/s^2)G(\tau_1, \tau_2)$. Our expression for the function G agrees with [36], upon setting $z = [(1-\tau_1)/(1-1/\tau_2)]$, $\bar{z} = [(1-1/\tau_1)/(1-\tau_2)]$.

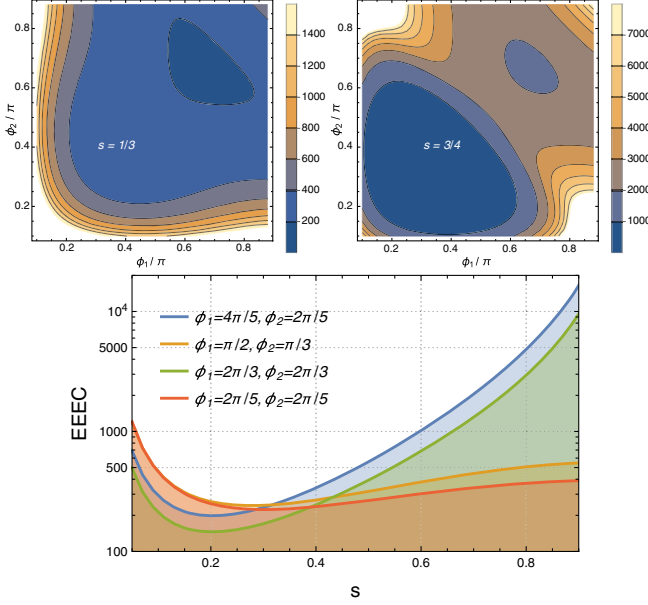


FIG. 3. EEEC at leading order in $\mathcal{N} = 4$ sYM. We display the function $H(s, \tau_1 = e^{i\phi_1}, \tau_2 = e^{i\phi_2})$ in various kinematic regions. Top: Distribution in (ϕ_1, ϕ_2) with $s = \text{constant}$. Bottom: Distribution in s with fixed (ϕ_1, ϕ_2) .

The “squeezed limit” corresponds to the regime where we put two detectors on top of each other, $\zeta_{12} \sim 0$, $\zeta_{13} \sim \zeta_{23} \sim \zeta$. We can access this limit by taking $\tau_2 \rightarrow 1$, keeping s, τ_1 fixed, and we find that the leading-power contributions can be grouped into a simple form:

$$H^{\zeta_{12} \rightarrow 0} \sim \frac{6}{\zeta_{12}} \left[\frac{\zeta + \ln(1 - \zeta)}{(-1 + \zeta)\zeta^3} \right], \quad (23)$$

where the coefficient of the leading pole depends on a single variable: $\zeta = -[s(1 - \tau_1)^2 / (1 + s)^2 \tau_1]$.

The “coplanar limit” corresponds to the surface where Δ_1 vanishes. In this regime, a soft particle recoils against three coplanar hard particles, which are scattered into two different half-planes. We extract the leading singular behavior by expanding the function H around $s = 1$, recalling $\tau_1 = e^{i\phi_1}$, $\tau_2 = e^{i\phi_2}$,

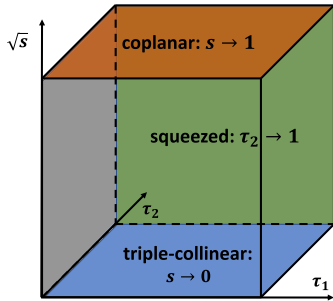


FIG. 4. Kinematic regions for the EEEC and its singular regimes.

$$H^s \sim 18\pi \frac{\theta(-\cos \frac{\phi_1}{2} \cos \frac{\phi_2}{2} \cos \frac{\phi_1 + \phi_2}{2})}{[\sin \frac{\phi_1}{2} \sin \frac{\phi_2}{2} \sin \frac{\phi_1 + \phi_2}{2}]^3} \times \frac{1}{|1 - s|} \ln \left[(1 - s)^2 \tan^2 \frac{\phi_1}{2} \tan^2 \frac{\phi_2}{2} \tan^2 \frac{\phi_1 + \phi_2}{2} \right]. \quad (24)$$

The pole at $s = 1$ comes solely from the discontinuity of the g_8 function in the region where $-w_i$ sit on the negative real axis. The physical origin of the leading logarithms is soft-collinear singularity. Lifting the result to $(4 - 2\epsilon)$ —dimension, Eq. (24) can be recast into distributional terms including $\delta(1 - s)$ and plus distributions [63]. The ϵ —IR divergences in the delta function cancels with those coming from the one-loop virtual contribution [49], making the event shape finite at $s = 1$.

Since the $s \rightarrow 1$ behavior of the EEEC in $\mathcal{N} = 4$ sYM is analogous to that in QCD, we anticipate that the leading Sudakov logarithms that appear in both theories are the same, which can be resummed to all loop orders [27].

Outlook.—Our work opens the way for several applications and further studies. Our one-loop formula, Eq. (16), constitutes the first analytic result for a event-shape observable living in a three-dimensional parameter space. Its symbol defines a set of 16 rational alphabet letters describing a finite physical observable. By embedding the kinematic space in a hexagon located on a unit circle, we identify the symmetry properties and first-entry conditions that provide key information on the function space. Further studies on these mathematical structures and analytic properties will be crucial for bootstrapping the observable at higher perturbative order in supersymmetric gauge theories or in QCD.

In addition to the leading asymptotic behaviors we provide, our result contains information about subleading powers as well. The data in the triple-collinear, squeezed, and coplanar limits will shed new light on corresponding operator product expansion limits of the light-ray operators [64], thus making it possible to understand these limits at arbitrary coupling [65,66]. In the meantime, the analysis in each aforementioned kinematic limit can be generalized to QCD, providing rich content for theoretical and phenomenological studies, as major progress has been achieved in the triple-collinear limit [67–70].

Our approach to compute the EEEC in $\mathcal{N} = 4$ sYM benefits from the simplicity of the squared super form factor, which allows an integral representation in a concise form. As novel research ideas emerged in recent studies on the form factors by means of harmonic superspace formalism [71–73], modern amplitude techniques [74–77], and integrability descriptions [78–80], they open the way to probing the energy correlator observable at higher loop order or finite coupling, as well as relevant generalization of the event shape in quantum field theories [11,81–84].

We are grateful to Dmitry Chicherin, Gregory Korchemsky, Emery Sokatchev, and Alexander Zhiboedov

for initiations and generous help with the calculation. We acknowledge enlightening discussions with Hao Chen, Johannes Henn, Yibei Li, Ian Moulton, Alexander Tumanov, Tong-Zhi Yang, and Hua Xing Zhu. In its early stage, the work received funding from the European Research Council (ERC) under the European Union's Horizon 2020 research and innovation program, "Novel structures in scattering amplitudes" (grant agreement no. 725110).

-
- [1] E. Coleman, M. Freytsis, A. Hinzmann, M. Narain, J. Thaler, N. Tran, and C. Vernieri, *J. Instrum.* **13**, T01003 (2018).
- [2] A. J. Larkoski, I. Moulton, and B. Nachman, *Phys. Rep.* **841**, 1 (2020).
- [3] L. Asquith *et al.*, *Rev. Mod. Phys.* **91**, 045003 (2019).
- [4] P. T. Komiske, E. M. Metodiev, and J. Thaler, *J. High Energy Phys.* 01 (2019) 121.
- [5] S. Marzani, G. Soyez, and M. Spannowsky, *Lect. Notes Phys.* **958**, 23 (2019).
- [6] K. Datta, A. Larkoski, and B. Nachman, *Phys. Rev. D* **100**, 095016 (2019).
- [7] T. Kinoshita, *J. Math. Phys. (N.Y.)* **3**, 650 (1962).
- [8] T. D. Lee and M. Nauenberg, *Phys. Rev.* **133**, B1549 (1964).
- [9] D. M. Hofman and J. Maldacena, *J. High Energy Phys.* 05 (2008) 012.
- [10] N. Arkani-Hamed and J. Maldacena, [arXiv:1503.08043](https://arxiv.org/abs/1503.08043).
- [11] G. Korchemsky, E. Sokatchev, and A. Zhiboedov, [arXiv:2106.14899](https://arxiv.org/abs/2106.14899).
- [12] C. L. Basham, L. S. Brown, S. D. Ellis, and S. T. Love, *Phys. Rev. Lett.* **41**, 1585 (1978).
- [13] L. J. Dixon, M.-X. Luo, V. Shtabovenko, T.-Z. Yang, and H. X. Zhu, *Phys. Rev. Lett.* **120**, 102001 (2018).
- [14] M.-X. Luo, V. Shtabovenko, T.-Z. Yang, and H. X. Zhu, *J. High Energy Phys.* 06 (2019) 037.
- [15] A. V. Belitsky, S. Hohenegger, G. P. Korchemsky, E. Sokatchev, and A. Zhiboedov, *Phys. Rev. Lett.* **112**, 071601 (2014).
- [16] J. M. Henn, E. Sokatchev, K. Yan, and A. Zhiboedov, *Phys. Rev. D* **100**, 036010 (2019).
- [17] D. G. Richards, W. J. Stirling, and S. D. Ellis, *Phys. Lett.* **119B**, 193 (1982).
- [18] D. G. Richards, W. J. Stirling, and S. D. Ellis, *Nucl. Phys.* **B229**, 317 (1983).
- [19] A. Ali and F. Barreiro, *Phys. Lett.* **118B**, 155 (1982).
- [20] N. K. Falck and G. Kramer, *Z. Phys. C* **42**, 459 (1989).
- [21] Z. Kunszt, P. Nason, G. Marchesini, and B. R. Webber, in *LEP Physics Workshop Geneva, Switzerland, 1989* (1989), pp. 373–453, https://inis.iaea.org/collection/NCLCollectionStore/_Public/21/009/21009162.pdf.
- [22] E. W. N. Glover and M. R. Sutton, *Phys. Lett. B* **342**, 375 (1995).
- [23] K. A. Clay and S. D. Ellis, *Phys. Rev. Lett.* **74**, 4392 (1995).
- [24] G. Kramer and H. Spiesberger, *Z. Phys. C* **73**, 495 (1997).
- [25] V. Del Duca, C. Duhr, A. Kardos, G. Somogyi, and Z. Trócsányi, *Phys. Rev. Lett.* **117**, 152004 (2016).
- [26] V. Del Duca, C. Duhr, A. Kardos, G. Somogyi, Z. Szőr, Z. Trócsányi, and Z. Tulipánt, *Phys. Rev. D* **94**, 074019 (2016).
- [27] J. C. Collins and D. E. Soper, *Nucl. Phys.* **B193**, 381 (1981); **B213**, 545(E) (1983).
- [28] J. Kodaira and L. Trentadue, *Phys. Lett.* **112B**, 66 (1982).
- [29] D. de Florian and M. Grazzini, *Nucl. Phys.* **B704**, 387 (2005).
- [30] Z. Tulipánt, A. Kardos, and G. Somogyi, *Eur. Phys. J. C* **77**, 749 (2017).
- [31] I. Moulton and H. X. Zhu, *J. High Energy Phys.* 08 (2018) 160.
- [32] I. Moulton, G. Vita, and K. Yan, *J. High Energy Phys.* 07 (2020) 005.
- [33] K. Konishi, A. Ukawa, and G. Veneziano, *Phys. Lett.* **78B**, 243 (1978).
- [34] K. Konishi, A. Ukawa, and G. Veneziano, *Phys. Lett.* **80B**, 259 (1979).
- [35] L. J. Dixon, I. Moulton, and H. X. Zhu, *Phys. Rev. D* **100**, 014009 (2019).
- [36] H. Chen, M.-X. Luo, I. Moulton, T.-Z. Yang, X. Zhang, and H. X. Zhu, *J. High Energy Phys.* 08 (2020) 028.
- [37] N. A. Sveshnikov and F. V. Tkachov, *Phys. Lett. B* **382**, 403 (1996).
- [38] G. P. Korchemsky, G. Oderda, and G. F. Sterman, *AIP Conf. Proc.* **407**, 988 (1997).
- [39] G. P. Korchemsky and G. F. Sterman, *Nucl. Phys.* **B555**, 335 (1999).
- [40] A. V. Belitsky, G. P. Korchemsky, and G. F. Sterman, *Phys. Lett. B* **515**, 297 (2001).
- [41] A. V. Belitsky, S. Hohenegger, G. P. Korchemsky, E. Sokatchev, and A. Zhiboedov, *Nucl. Phys.* **B884**, 206 (2014).
- [42] A. V. Belitsky, S. Hohenegger, G. P. Korchemsky, and E. Sokatchev, *Nucl. Phys.* **B904**, 176 (2016).
- [43] G. P. Korchemsky and E. Sokatchev, *J. High Energy Phys.* 12 (2015) 133.
- [44] B. Eden, P. Heslop, G. P. Korchemsky, and E. Sokatchev, *Nucl. Phys.* **B869**, 329 (2013).
- [45] B. Eden, P. Heslop, G. P. Korchemsky, and E. Sokatchev, *Nucl. Phys.* **B869**, 378 (2013).
- [46] J. M. Henn, *Annu. Rev. Nucl. Part. Sci.* **71**, 87 (2021).
- [47] W. L. van Neerven, *Z. Phys. C* **30**, 595 (1986).
- [48] L. V. Bork, D. I. Kazakov, and G. S. Vartanov, *J. High Energy Phys.* 02 (2011) 063.
- [49] L. V. Bork, D. I. Kazakov, and G. S. Vartanov, *J. High Energy Phys.* 10 (2011) 133.
- [50] B. Penante, B. Spence, G. Travaglini, and C. Wen, *J. High Energy Phys.* 04 (2014) 083.
- [51] A. Brandhuber, O. Gürdogan, R. Mooney, G. Travaglini, and G. Yang, *J. High Energy Phys.* 10 (2011) 046.
- [52] L. Bianchi, A. Brandhuber, R. Panerai, and G. Travaglini, *J. High Energy Phys.* 02 (2019) 182.
- [53] D. Chicherin, G. Korchemsky, and E. Sokatchev (to be published).
- [54] A. Gehrmann-De Ridder, T. Gehrmann, and G. Heinrich, *Nucl. Phys.* **B682**, 265 (2004).
- [55] F. Brown, *Commun. Math. Phys.* **287**, 925 (2009).
- [56] F. C. S. Brown, [arXiv:0910.0114](https://arxiv.org/abs/0910.0114).
- [57] C. Bogner and M. Luders, *Contemp. Math.* **648**, 11 (2015).

- [58] E. Panzer, Feynman integrals and hyperlogarithms, Ph.D. thesis, Humboldt University, Berlin, Inst. Math., 2015.
- [59] E. Panzer, *Comput. Phys. Commun.* **188**, 148 (2015).
- [60] J. Golden, M. F. Paulos, M. Spradlin, and A. Volovich, *J. Phys. A* **47**, 474005 (2014).
- [61] J. Golden and A. J. McLeod, *J. High Energy Phys.* **01** (2019) 017.
- [62] L. J. Dixon, C. Duhr, and J. Pennington, *J. High Energy Phys.* **10** (2012) 074.
- [63] I. M. Gelfand and G. E. Shilov, *Generalized Functions. Vol. 1, Properties and Operations* (Academic Press, New York, NY, USA, 1964).
- [64] P. Kravchuk and D. Simmons-Duffin, *J. High Energy Phys.* **11** (2018) 102.
- [65] C.-H. Chang and D. Simmons-Duffin, [arXiv:2202.04090](https://arxiv.org/abs/2202.04090).
- [66] H. Chen, I. Moulton, J. Sandor, and H. X. Zhu, [arXiv:2202.04085](https://arxiv.org/abs/2202.04085).
- [67] H. Chen, I. Moulton, and H. X. Zhu, *Phys. Rev. Lett.* **126**, 112003 (2021).
- [68] H. Chen, I. Moulton, and H. X. Zhu, [arXiv:2104.00009](https://arxiv.org/abs/2104.00009).
- [69] H. Chen, I. Moulton, X. Y. Zhang, and H. X. Zhu, *Phys. Rev. D* **102**, 054012 (2020).
- [70] P. T. Komiske, I. Moulton, J. Thaler, and H. X. Zhu, [arXiv:2201.07800](https://arxiv.org/abs/2201.07800).
- [71] D. Chicherin and E. Sokatchev, *J. High Energy Phys.* **02** (2017) 062.
- [72] D. Chicherin and E. Sokatchev, *J. High Energy Phys.* **03** (2017) 048.
- [73] D. Chicherin, G. Korchemsky, and E. Sokatchev (to be published).
- [74] G. Lin, G. Yang, and S. Zhang, [arXiv:2112.09123](https://arxiv.org/abs/2112.09123).
- [75] Y. Guo, L. Wang, and G. Yang, *Phys. Rev. Lett.* **127**, 151602 (2021).
- [76] L. J. Dixon, A. J. McLeod, and M. Wilhelm, *J. High Energy Phys.* **04** (2021) 147.
- [77] L. J. Dixon, O. Gurdogan, A. J. McLeod, and M. Wilhelm, *Phys. Rev. Lett.* **128**, 111602 (2022).
- [78] A. Sever, A. G. Tumanov, and M. Wilhelm, *Phys. Rev. Lett.* **126**, 031602 (2021).
- [79] A. Sever, A. G. Tumanov, and M. Wilhelm, *J. High Energy Phys.* **10** (2021) 071.
- [80] A. Sever, A. G. Tumanov, and M. Wilhelm, *J. High Energy Phys.* **03** (2022) 128.
- [81] I. Moulton, L. Necib, and J. Thaler, *J. High Energy Phys.* **12** (2016) 153.
- [82] P. T. Komiske, E. M. Metodiev, and J. Thaler, *J. High Energy Phys.* **04** (2018) 013.
- [83] R. S. Chivukula, K. A. Mohan, D. Sengupta, and E. H. Simmons, *J. High Energy Phys.* **03** (2018) 133.
- [84] A. Martin and J.-M. Richard, *Phys. Rev. D* **101**, 094014 (2020).
- [85] See Supplemental Material at <http://link.aps.org/supplemental/10.1103/PhysRevLett.129.021602> for the main result of this letter: the analytic expression for EEEEC with full angular dependence.